Geochemistry Geophysics Geosystems G3
AN ELECTRONIC JOURNAL OF THE EARTH SCIENCES
Published by AGU and the Geochemical Society

Article
Volume 10, Number 3
11 March 2009
Q03007, doi:10.1029/2008GC002196
ISSN: 1525-2027

Southern African continental margin: Dynamic processes of a transform margin

N. Parsiegla
Alfred Wegener Institute for Polar and Marine Research, P.O. Box 120161, D-27515 Bremerhaven, Germany

Now at RWE Dea AG, Überseering 40, D-22297 Hamburg, Germany (nicole.parsiegla@rwe.com)

J. Stankiewicz
GeoForschungsZentrum Potsdam, Telegrafenberg, D-14473 Potsdam, Germany

K. Gohl
Alfred Wegener Institute for Polar and Marine Research, P.O. Box 120161, D-27515 Bremerhaven, Germany

T. Ryberg
GeoForschungsZentrum Potsdam, Telegrafenberg, D-14473 Potsdam, Germany

G. Uenzelmann-Neben
Alfred Wegener Institute for Polar and Marine Research, P.O. Box 120161, D-27515 Bremerhaven, Germany

[1] Dynamic processes at sheared margins associated with the formation of sedimentary basins and marginal ridges are poorly understood. The southern African margin provides an excellent opportunity to investigate the deep crustal structure of a transform margin and to characterize processes acting at these margins by studying the Agulhas-Falkland Fracture Zone, the Outeniqua Basin, and the Diaz Marginal Ridge. To do this, we present the results of the combined seismic land-sea experiments of the Agulhas-Karoo Geoscience Transect. Detailed velocity-depth models show crustal thicknesses varying from ~42 km beneath the Cape Fold Belt to ~28 km beneath the shelf. The Agulhas-Falkland Fracture Zone is embedded in a 50 km wide transitional zone between continental and oceanic crust. The oceanic crust farther south exhibits relatively low average crustal velocities (~6.0 km/s), which can possibly be attributed to transform-ridge intersection processes and the thermal effects of the adjacent continental crust during its formation. Crustal stretching factors derived from the velocity-depth models imply that extension in the Outeniqua Basin acted on regional as well as more local scales. We highlight evidence for two episodes of crustal stretching. The first, with a stretching factor β of 1.6, is interpreted to have influenced the entire Outeniqua Basin. The stresses possibly originated from the beginning breakup between Africa and Antarctica (~169–155 Ma). The second episode can be associated with a transtensional component of the shear motion along the Agulhas-Falkland Transform from ~136 Ma. This episode caused additional crustal stretching with β = 1.3 and is established to only have affected the southern parts of the basin. Crustal velocities directly beneath the Outeniqua Basin are consistent with the interpretation of Cape Supergroup rocks underlying most parts of the basin and the Diaz Marginal Ridge. We propose that the formation of this ridge can be either attributed to a transpressional episode along the Agulhas-Falkland Transform or, more likely, to thermal uplift accompanying the passage of a spreading ridge to the south.

Components: 10,769 words, 10 figures, 5 tables.

Keywords: sheared margin/transform margin; crustal stretching; fracture zone; plate tectonics; Agulhas-Karoo Geoscience Transect; seismic refraction/reflection.

Index Terms: 8106 Tectonophysics: Continental margins: transform; 3025 Marine Geology and Geophysics: Marine seismics (0935, 7294); 9305 Geographic Location: Africa.

Received 31 July 2008; **Revised** 18 December 2008; **Accepted** 12 January 2009; **Published** 11 March 2009.

Parsiegla, N., J. Stankiewicz, K. Gohl, T. Ryberg, and G. Uenzelmann-Neben (2009), Southern African continental margin: Dynamic processes of a transform margin, *Geochem. Geophys. Geosyst.*, *10*, Q03007, doi:10.1029/2008GC002196.

1. Introduction

[2] The southern African margin is a transform margin which developed as a result of the relative motion between Africa and South America along the Agulhas-Falkland Transform Fault which is conserved in the present Agulhas-Falkland Fracture Zone (AFFZ) (Figure 1). In general, such a sheared margin develops in three phases [*Bird*, 2001; *Lorenzo*, 1997] starting with the continent-continent stage (rift stage) in which a continental shear zone develops, such as the San Andreas [e.g., *Furlong and Hugo*, 1989] or Dead Sea faults [e.g., *Pe'eri et al.*, 2002]. Following the onset of seafloor spreading at a neighboring stretched margin segment, oceanic crust slides past the continental crust on the sheared margin, which is now in its continent-ocean shear stage (drift stage). The transform margin becomes inactive in its post shear stage, a term usually used for the southern African margin [*Scrutton*, 1976, 1979]. Although in this sense the AFFZ is no longer an active plate boundary, there are several indications for neotectonic processes whose causes are still under discussion (Figure 1) [*Ben-Avraham*, 1995; *Ben-Avraham et al.*, 1995; *Parsiegla et al.*, 2007].

[3] The AFFZ stretches from the northern boundary of the Falkland Plateau through the south Atlantic to the southern boundary of the African continent (Figure 2) and had an original transform offset of 1200 km [*Ben-Avraham et al.*, 1997]. North of the fracture zone, the Outeniqua Basin (Figure 3) consists of a set of small fault-bounded subbasins in the north and a distinctively deeper subbasin (the Southern Outeniqua Basin) in the vicinity of the AFFZ. The cause of this variability, the amount of stretching, and the structure of the crust underlying the basins and the AFFZ, are not understood. There is also an ongoing discussion about whether these basins are underlain by rocks of the Cape Fold Belt (Figure 1) [e.g., *Broad et al.*, 2006; *McMillan et al.*, 1997; *Thomson*, 1999] and, if so, whether the belt's structures had an impact on basin formation. As the basins are close to the AFFZ it is also possible that the shear process itself had an influence on basin geometry and sedimentation processes. Plate tectonic reconstructions [*Eagles*, 2007; *König and Jokat*, 2006; *Martin et al.*, 1982] show that the sedimentary basins of the Falkland Plateau (Figure 2) were conjugate to the Outeniqua Basin before Gondwana breakup, which leads to the question to what extent these basins have shared histories.

[4] In order to find answers to these questions and to understand the processes that shaped this margin and its structures, the Alfred Wegener Institute for Polar and Marine Research (AWI) and the Geoforschungszentrum Potsdam (GFZ) acquired seismic refraction/wide-angle reflection data along two combined onshore-offshore profiles across the southern continental margin of South Africa [*Uenzelmann-Neben*, 2005] (Figure 1). Parts of these profiles are published by *Parsiegla et al.* [2007, 2008] and *Stankiewicz et al.* [2007, 2008]. In this study, we present both profiles at their full lengths (Table 1) and incorporate as yet unpublished data. In the following, we will refer to these combined land-sea profiles, which are part of the Agulhas-Karoo Geoscience Transect in the German–South African cooperation program Inkaba yeAfrica [*de Wit and Horsfield*, 2006], as the eastern profile (AWI-20050200-GRA) and western profile (AWI-20050100-FRA) (Figures 1 and 3).

2. Geological and Tectonic Background

[5] Southern Africa experienced a 3.8 billion year long geological history of continental accretion and disassembly [*Tankard et al.*, 1982]. Here, we restrict the review of the relevant geological and

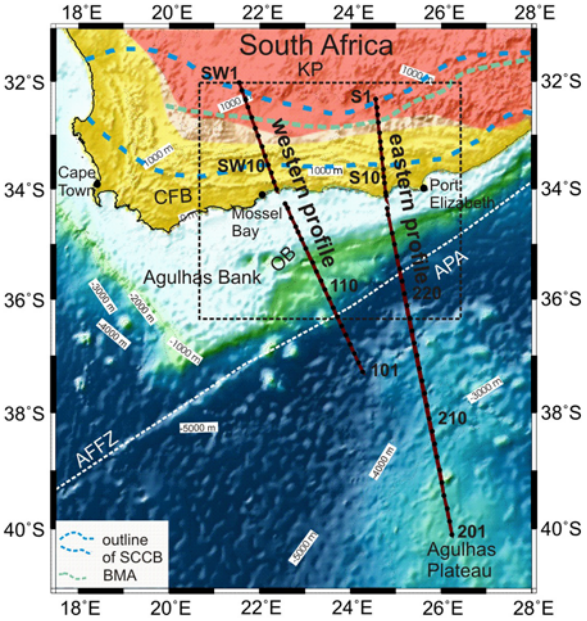

Figure 1. Overview map of the investigation area with the satellite derived topography [*Smith and Sandwell*, 1997] showing the location of both combined onshore-offshore seismic profiles (western profile and eastern profile) of the Agulhas-Karoo Geoscience Transect. Brown lines represent the profile location, dots in the onshore part are positions of land shots, and dots in the offshore part are positions of ocean bottom seismometers (OBS). Some shot positions (SW for the western profile and S for the eastern profile) and OBS positions are labeled for orientation. The locations of seismic land stations are not plotted in Figure 1 but can be found in Figure 5. The Agulhas-Falkland Fracture Zone (AFFZ) is marked with a dashed white line. The Cape Fold Belt (CFB) is shown as a yellow area, and the Karoo Province (KP) is shown in light red on the map. The position of the Southern Cape Conductivity Belt (SCCB) is outlined by a blue dashed line, and the Beattie Magnetic Anomaly (BMA) is sketched by a green line (positions after *de Beer et al.* [1982]). The dashed box shows the position of the detail map of the onshore geology and structure of the offshore basins (Figure 3). APA, Agulhas Passage; OB, Outeniqua Basin.

tectonic processes to the last ~450 Ma, starting with the deposition of Cape Fold Belt rocks (CFB) and the Karoo Basin (Figure 1). The Cape Supergroup (Figure 3) was deposited between 450 and 300 Ma during a series of transgression-regression cycles [*Hälbich*, 1993; *Tankard et al.*, 1982]. Between 278 and 215 Ma, these strata were folded by reactivation of pan-African thrusts to form the CFB [*Hälbich*, 1993; *Hälbich et al.*, 1983]. The CFB formed part of a single major fold belt that developed during the Gondwanide Orogeny, along with the Sierra de la Ventana (eastern Argentina) and Pensacola Mountains (East Antarctica) and the Ellsworth Mountains (West Antarctica) [e.g., *Vaughan and Pankhurst*, 2008]. The cause of this orogeny is a subject of ongoing debate. While many authors favor flat slab subduction of the proto-Pacific plate beneath Gondwana [e.g., *Lock*, 1980], others find supporting arguments for collision [*Pankhurst et al.*, 2006] or dextral transpressional scenarios [*Johnston*, 2000]. During late Carboniferous and early Jurassic times, the Karoo Supergroup (Figure 3 [*Cole*, 1992]) was deposited in the Karoo basin, the foreland basin of the CFB. Sedimentation ended with the extrusion of basaltic lavas [*Cole*, 1992] to form the Karoo Large Igneous Province at 183 ± 1 Ma [*Duncan et al.*, 1997]. This volcanism has been attributed to the Bouvet plume [*Hawkesworth et al.*, 1999], and accompanied the first movements between eastern and western parts of Gondwana [*Eagles and König*, 2008].

[6] In mid-late Jurassic times, rifting processes started to form the horst, graben and half-graben structures of the Outeniqua Basin [*Broad et al.*, 2006; *McMillan et al.*, 1997]. This basin (Figure 3) consists of a complex system of subbasins separated from each other by faults and basement arches [*Broad et al.*, 2006; *McMillan et al.*, 1997]. The subbasins, from west to east, are the Bredasdorp, Infanta, Pletmos, Gamtoos, and Algoa basins and their deep, southern extension the Southern Outeniqua Basin (SOB, Figures 3 and 4). *Broad et al.* [2006] divides the sedimentary fill of these basins into synrift and drift sequences, related to their development during a phase of active rifting that was followed by passive subsidence following the separation of the Falkland Plateau from the South African margin. The Diaz Marginal Ridge (DMR, Figure 3) separates the sedimentary basins from the Agulhas-Falkland Fracture Zone (AFFZ, Figures 1–3), which is formed during right lateral strike-slip motion between South America and Africa in early Cretaceous times. *Ben-Avraham et al.* [1993] and *Thomson* [1999] show how shearing on the fracture zone caused local deformation in neighboring parts of the Outeniqua Basin.

[7] An episode of increased denudation accompanied Gondwana breakup in southern Africa, and may be related to epeirogenic uplift over an area of increased mantle buoyancy [*Tinker et al.*, 2008]. Another denudation (~uplift) episode took place between 100 and 80 Ma [*Tinker et al.*, 2008]. Both uplift episodes were accompanied by kimberlite

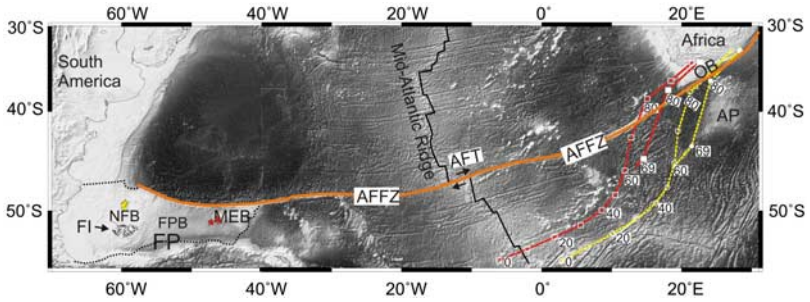

Figure 2. Map of the satellite derived bathymetry/topography by *Smith and Sandwell* [1997] showing the Agulhas-Falkland Fracture Zone (orange line) and bordering continents. The tracks of the Shona (red lines, with filled squares [*Martin*, 1987] and open squares [*Hartnady and le Roex*, 1985]) and Bouvet (yellow dashed lines, with filled circles [*Martin*, 1987] and with open circles [*Hartnady and le Roex*, 1985]) hot spots are shown. In the Falkland basins (NFB, North Falkland Basin; FPB, Falkland Plateau Basin) the locations of Deep Sea Drilling Project sites [*Jeletzky*, 1983; *Jones and Plafker*, 1977] are marked with red stars, and hydrocarbon exploration drill holes are marked with yellow stars [*Richards and Hillier*, 2000]. AP, Agulhas Plateau; AFT, present-day position of the Agulhas-Falkland Transform; OB, Outeniqua Basin; FP, Falkland Plateau; FI, Falkland Islands; MEB, Maurice Ewing Bank.

emplacement and the formation of Large Igneous Provinces [*Tinker et al.*, 2008]. The latter uplift phase occurred when the Agulhas Plateau Large Igneous Province formed 100–94 Ma ago [*Gohl and Uenzelmann-Neben*, 2001; *Parsiegla et al.*, 2008; *Uenzelmann-Neben et al.*, 1999]. The interplay of uplift, mantle buoyancy, igneous activity, and continental breakup has led to the present-day appearance of southern Africa and its continental margin.

3. Seismic Data Acquisition, Processing, and Modeling

[8] Three types of data sets were acquired along both profiles (Figure 1), those from (1) air gun shots recorded by ocean bottom seismometers (OBS) [*Parsiegla et al.*, 2007, 2008], (2) air gun shots recorded at onshore seismic stations equipped with a GPS synchronized electronic data logger and a three-component seismometer (this study), and (3) land shots (twin explosives of 75–125 kg each) recorded with seismic land stations [*Stankiewicz et al.*, 2007]. Land shots could not be identified in the OBS records. The settings for the two profiles are summarized in Table 1. In this study, we present a new combined onshore-offshore model of the eastern profile and compare it with results from the western profile [*Stankiewicz et al.*, 2008]. Data examples for the eastern profile are shown in Figure 5 (see auxiliary material for more data examples) and explanations of phase names are given in Table 2.[1]

[1]Auxiliary materials are available in the HTML. doi:10.1029/2008GC002196.

[9] P wave traveltimes of air gun shots recorded at land stations, which have not been published before, were identified and added to the data sets of *Parsiegla et al.* [2008] and *Stankiewicz et al.* [2007]. Their data include P wave traveltime information from air gun shots recorded by ocean bottom seismometers and from land shots recorded at seismic land stations. We set pick uncertainties in the range from 40 ms to 150 ms, depending on the signal-to-noise ratio, and used the RAYINVR ray tracing and traveltime inversion routine of *Zelt and Smith* [1992] for modeling. The onshore [*Stankiewicz et al.*, 2007] and offshore [*Parsiegla et al.*, 2008] velocity-depth models were combined in a joint model of the velocity-depth structure over the continental margin of southern Africa from the Karoo basin to the Agulhas Plateau (Figure 1 and Table 1). We extended this initial model with the additional data from the air gun shots recorded at land stations. The resulting velocity-depth model of the eastern profile is shown in Figure 6. This P wave velocity-depth model consists of 6 layers, where the crust is represented by four layers (layers 1–4), and the mantle by two layers (layers 5–6). The first layer of the crust (sedimentary rocks) only exists in the offshore part of the profile. Results from seismic reflection measurements (e.g., Figure 4) were used to assign the thickness of this layer [*Parsiegla et al.*, 2008].

[10] The quality of our P wave velocity-depth model is assessed with the tools of RAYINVR [*Zelt and Smith*, 1992]. We obtained very good fits between modeled and measured traveltimes (Figure 5). The modeled traveltimes of the eastern profile have an overall RMS traveltime deviation of 0.141 s and χ^2 of 1.154 (see Table 3 for details

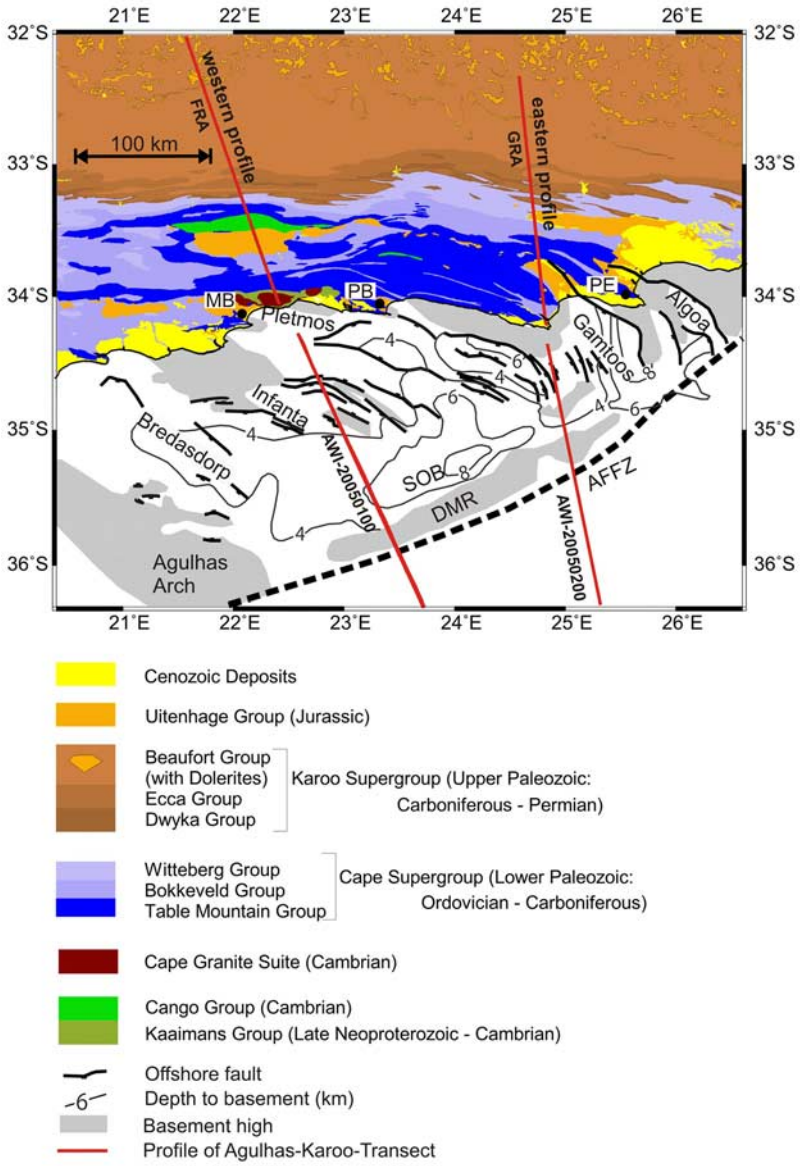

Figure 3. Detail map of the onshore geology and structure of the offshore basins. The locations of dominant faults and the depth-to-basement information of the Outeniqua Basin and its subbasins (Bredasdorp, Infanta, Pletmos, Gamtoos, Algoa, and Southern Outeniqua Basin) were adopted from *South African Agency for Promotion of Petroleum Exploration and Exploitation* [2003]. The onshore geology available from the AEON Africa database [*de Wit and Stankiewicz*, 2006] was included. FRA/GRA and AWI-20050100/200 are the names of the onshore and offshore subprofiles of the western and eastern profile, respectively. The dashed line marks the position of the Agulhas-Falkland Fracture Zone (AFFZ). DMR, Diaz Marginal Ridge; MB, Mossel Bay; PB, Plettenberg Bay; PE, Port Elizabeth; SOB, Southern Outeniqua Basin.

of the statistics). Most parts of the velocity-depth model are well constrained by a good ray coverage (Figure 7a). Regions of low ray coverage exist between 300 and 350 km profile distance in the lower crust (layer 4), between 150 and 300 km in the upper mantle (layer 5) and at the model limits. The model resolution was calculated at the depth (Figure 7b) and velocity nodes (Figure 7c). Nodes with a resolution of greater than 0.5 (within a range of 0 to 1) are considered well resolved [*Zelt and White*, 1995]. This condition is fulfilled for most of the depth nodes of the model (Figure 7b, blue circles) except for small areas of low ray coverage. These poorly resolved boundary nodes are mostly found in the regions of 300–350 km (base layer 2, 3, and 4) and 660–780 km profile distance (base

Table 1. Description of Sources, Receivers, Lengths, and Positions of the Offshore Seismic Refraction Profiles AWI-20050100 and AWI-20050200 and the Onshore Seismic Refraction Profiles FRA and GRA, Which Are Parts of the Western and Eastern Combined Onshore-Offshore Profiles[a]

	Western Profile		Eastern Profile	
	AWI-20050100	FRA	AWI-20050200	GRA
Source description	eight G. Guns™, one Bolt air gun, V_{tot} = 96 L	twin explosives, 75–125 kg each	eight G. Guns™, one Bolt air gun, V_{tot} = 96 L	twin explosives, 75–125 kg each
Number of shots	4420	13	4761	13
Average shot spacing (km)	0.15	20	0.15	20
Number (type) of stations	20 (OBS)	48 (three-component seismometer)	27 (OBS)	48 (three-component seismometer)
Length of profile (km)	457	240	663	210
Start of profile	34.24525°S, 22.56826°E	32.01766°S, 21.56335°E	34.39750°S, 24.84840°E	32.32425°S, 24.58266°E
End of profile	37.45232°S, 24.38704°E	34.04344°S, 22.40620°E	40.20290°S, 26.30270°E	34.20247°S, 24.82166°E

[a] V_{tot} is the total volume of the air guns, which were used during the marine experiment. The ocean bottom seismometers (OBS) consisted of a three-component seismometer and a hydrophone.

layer 3 and 4). The base of layer 5 could only be resolved for the two nodes at 250 and 300 km profile distance. The velocity nodes are similarly well resolved. The gridded velocity resolution plot (Figure 7c) shows that velocity nodes are relatively well resolved with large zones of resolution larger than 0.5. Less resolved regions include the upper layers of the offshore part of the model, the land-sea transition, 100–120 km (layer 3), 150–180 km (layer 3), 190–210 km (layer 4), 300–350 km

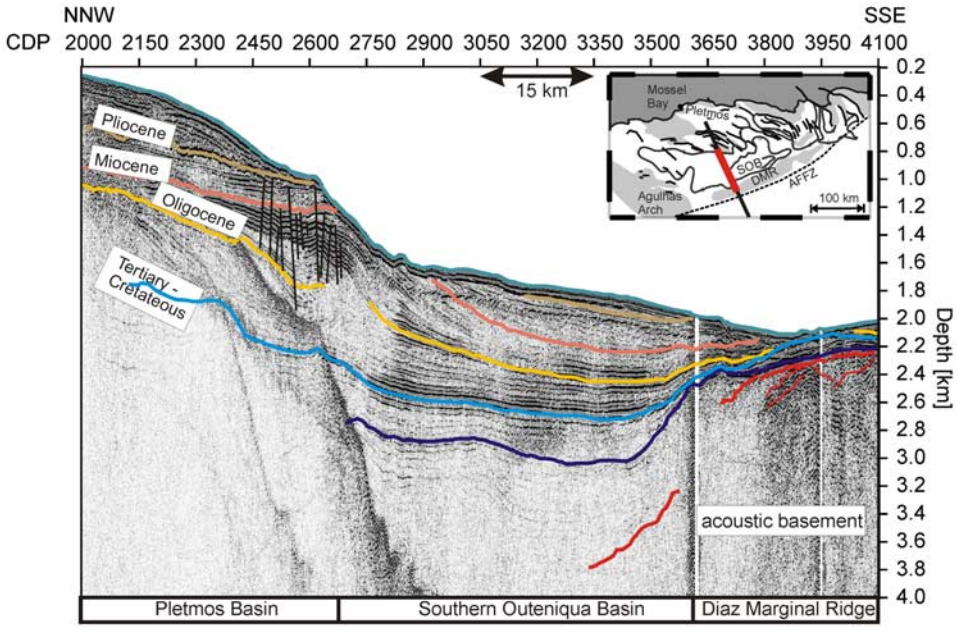

Figure 4. Depth migrated seismic reflection section AWI-20050200 (red straight line in the map) which is coincident to refraction line AWI-20050200 (black straight line in the map) and crosses the northern part of the Pletmos Basin, the Southern Outeniqua Basin, and the northern part of the Diaz Marginal Ridge. Seismic reflectors are marked with different colors, and reflector ages are annotated. Ages are based on the seismostratigraphic model of *Broad et al.* [2006]. For details on seismic reflection processing, see *Parsiegla et al.* [2007, 2008].

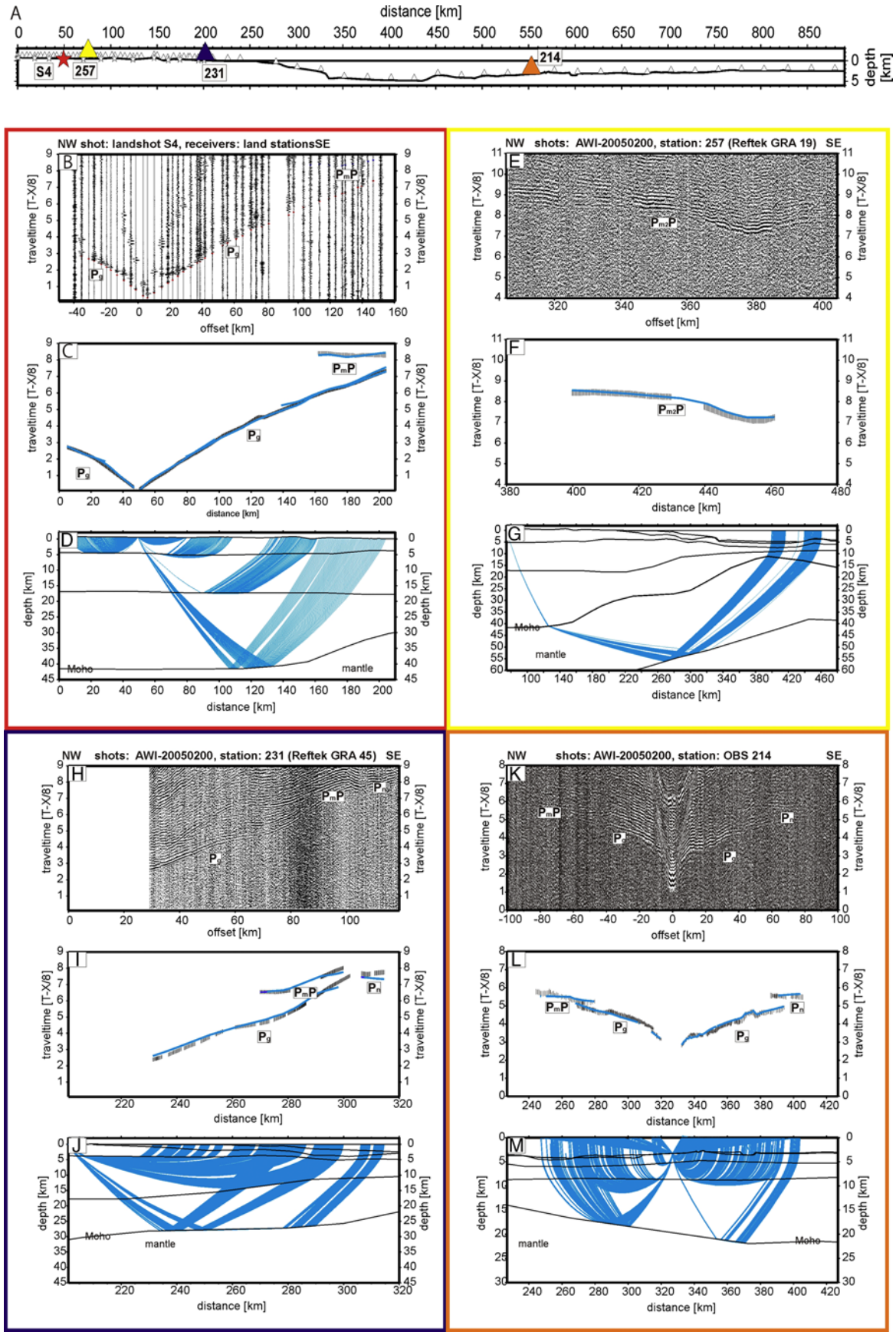
A
distance [km]
S4
257
231
214
depth [km]
NW shot: landshot S4, receivers: land stationsSE
B
C
D
traveltime [T-X/8]
offset [km]
distance [km]
depth [km]
Moho
mantle
NW shots: AWI-20050200, station: 257 (Reftek GRA 19) SE
E
F
G
NW shots: AWI-20050200, station: 231 (Reftek GRA 45) SE
H
I
J
NW shots: AWI-20050200, station: OBS 214 SE
K
L
M

Figure 5

Table 2. Names of Phases Identified in the Seismic P Wave Refraction Data Given Together With a Distinction Between Refracted and Reflected Phases and Their Origin in the Crust or Mantle

Name	Type	Origin
P_1	refracted P wave	model layer 1
Ps_1P	reflected P wave	top of model layer 2
Pg	refracted P wave	model layer 2, 3, 4
Pc_1P	reflected P wave	top of model layer 3
Pc_2P	reflected P wave	top of model layer 4
PmP	reflected P wave	top of model layer 5
Pn	refracted P wave	model layer 5
Pm2P	reflected P wave	top of model layer 6

(layer 4), and the northern and southern model limits.

4. Seismic Refraction and Wide-Angle Reflection Results and Implications

4.1. Velocity-Depth Structure Along the Eastern Profile and Comparison With the Western Profile

[11] The first crustal layer of the P wave velocity-depth model (Figure 6) represents sedimentary rocks with velocities between 1.7 and 3.4 km/s and a maximum thickness of 1.7 km in the shelf area (230–320 km profile distance). On the Agulhas Plateau (see also *Parsiegla et al.* [2008] for more information on this part of the profile), this sedimentary cover is thin or absent. The three crustal layers beneath the sedimentary layer differ in their seismic velocities and thicknesses in the northern part of the profile (0–290 km profile distance) compared to the southern part (350–890 km profile distance), which change over a 50–60 km wide transition zone centered on the AFFZ. Upper crustal seismic velocities are higher in the north (average 5.5 km/s) than in the south (average 5.0 km/s). A thick (up to 10 km) layer with seismic velocities above 7 km/s is observed in the lower crust of the southern part, while the lower crust in the north is characterized by average seismic velocities of 6.8 km/s.

[12] Crustal thickness (including the sedimentary layer) varies along the profile from 42 km beneath land, via 28 km in the shelf area and 8 km in the Agulhas Passage, to around 20 km on the Agulhas Plateau. Therefore, we observe distinct relief along the Mohorovièiæ discontinuity (Moho); between 150 and 200 km profile distance the Moho rises from 41 km to 29 km, and between 320 and 400 km it rises again from 27 to 12 km, before descending to 22 km further south.

[13] The western profile [see also *Stankiewicz et al.*, 2008] (Figures 1, 3, and 6) crosses similar variations. The shelf area, however, is 2.5 times wider than that on the eastern profile. A similar onshore crustal thickness, of 40 km, is observed, albeit with slightly higher seismic velocities (6.4–7.2 km/s) in the lower part of the crust (layer 4), especially at the southward decrease in Moho depth (140–250 km profile distance, 6.4–7.4 km/s) (Figure 6c). Both profiles exhibit a kink in the Moho starting at about 50 to 70 km inland from the coast and extending over a length of 50 to 60 km with a height difference of ~14 km. On both profiles, the transition zone between continental and oceanic crust is centered at the Agulhas-Falkland Fracture Zone with a width of ~50 km [*Parsiegla et al.*, 2007; this study].

4.2. Crustal Types Along the Eastern Profile

[14] According to the velocity-depth structure and the average velocities of the crystalline crust (Figures 6a and 6b), the profile can be subdivided into four units from north to south. For each unit, the thicknesses given are for the complete crustal column including the sedimentary layer but, for calculation of the average crustal velocity, the sedimentary layer was removed.

[15] From 0 to 300 km profile distance, the crust is about 42 km thick on the onshore part and about

Figure 5. Four data examples along the eastern onshore-offshore profile (AWI-200050200-GRA) are shown. (a) The positions of stations and land shots on the profile, where triangles mark station locations (land stations and ocean bottom seismometers (OBS)) and stars represent the location of land shots. The three stations and the shot whose data are shown are marked with a larger colored symbol where its color corresponds to the color of the box surrounding each set of illustrations. (b–d) Data of station 273 (landshot S4), (e–g) data of station 257 (GRA 19), (h–j) data of station 231 (GRA 45), and (k–m) data of station 214 (OBS). Figures 5b, 5e, 5h, and 5k plot the data itself; Figures 5c, 5f, 5i, and 5l plot the fits between measured and modeled traveltimes; and Figures 5d, 5g, 5j, and 5m plot the raypaths through the model. AWI-20050200 is the name of the air gun shot profile and the offshore seismic refraction profile, and GRA is the name of the onshore seismic refraction profile.

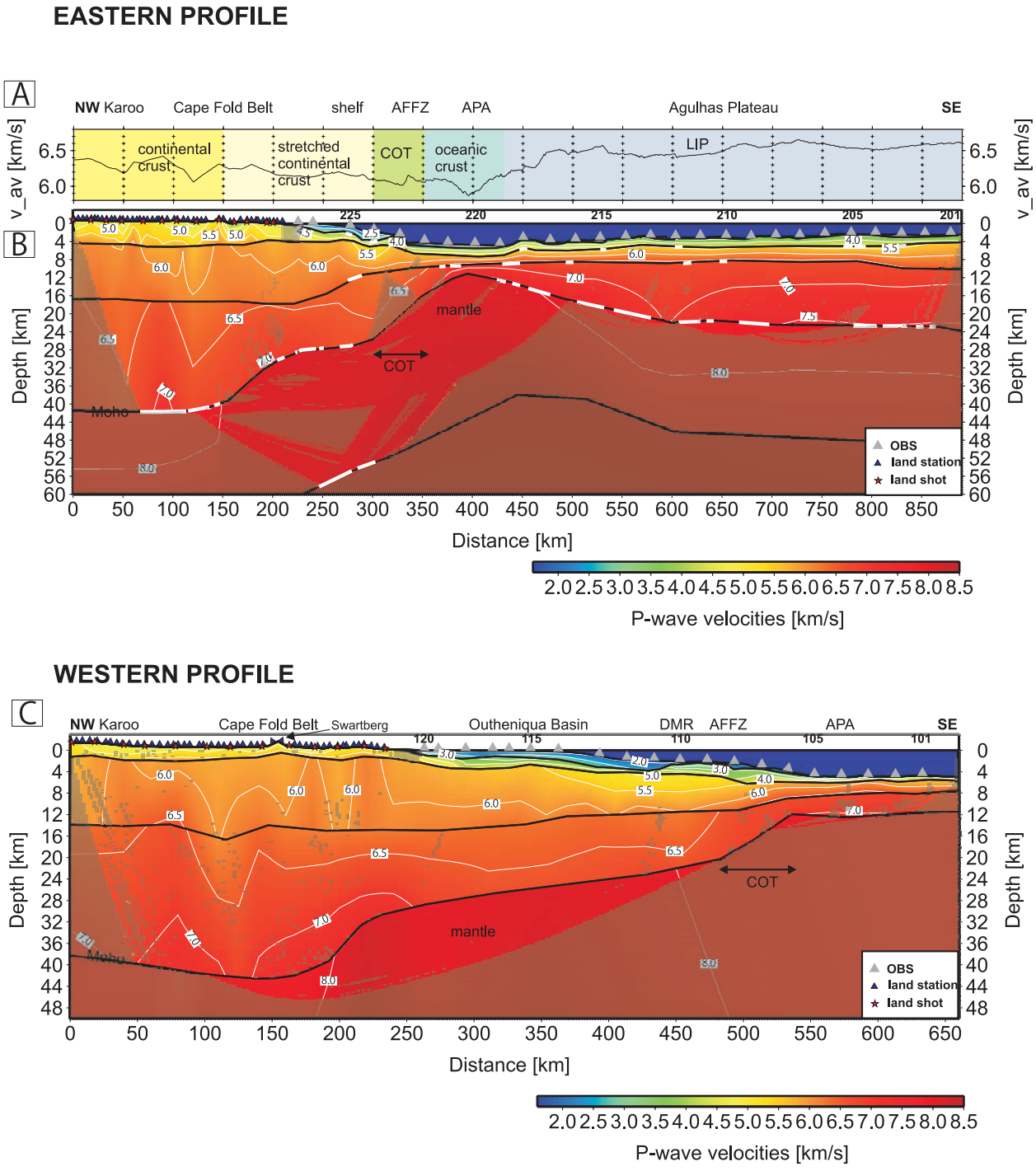

Figure 6. (a) Average velocities of the crust (without sedimentary layer) along the eastern onshore-offshore profile AWI-20050200-GRA with interpretation. (b) Seismic P wave velocity-depth model of the eastern profile. Gray triangles mark OBS positions, numbers over triangles indicate station numbers, blue triangles mark the positions of land stations, and red stars correspond to the positions of shots carried out onshore. Black lines represent model layer boundaries where thick white lines mark positions of reflected phases at these boundaries. Thin white lines are velocity isolines. Annotations on these lines in white boxes are velocities in km/s. Dark shaded areas are not covered by rays. AFFZ, Agulhas-Falkland Fracture Zone; APA, Agulhas Passage; COT, continent-ocean transition zone; LIP, Large Igneous Province. (c) Seismic P wave velocity-depth model of the western onshore-offshore profile AWI-20050100-FRA redrawn after *Stankiewicz et al.* [2008]. DMR, Diaz Marginal Ridge.

Table 3. Statistics of P Wave Traveltime Inversion[a]

Name	Picks	RMS	χ^2
P_1	56	0.077	1.113
Ps_1P	29	0.059	0.498
Pg	14720	0.117	0.986
Pc_1P	66	0.115	0.554
Pc_2P	131	0.081	0.554
PmP	1995	0.162	1.557
Pn	5224	0.189	1.559
Pm_2P	293	0.074	0.244
All	22514	0.141	1.154

[a] Number of traveltime picks, the root-mean-squared (rms) error of the fitting, and the χ^2 value of the different phases.

28 km on the shelf. These thicknesses are within the normal ranges for unstretched and stretched continental crust [e.g., *Christensen and Mooney*, 1995]. The onset of crustal thinning begins 50 km inland from the coast. Average crustal velocities of 6.29 km/s for the unstretched onshore part (0–150 km), 6.25 km/s for the stretched onshore part (150–200 km), and 6.15 km/s for the stretched offshore part (200–300 km) fall within the expected range for normal continental (felsic) crust [*Christensen and Mooney*, 1995]. The similar average (crystalline) crustal velocities for the stretched onshore and offshore continental crust suggest that rocks of the Cape Supergroup underlie the shelf area, consistent with results of drilling into basement highs of the Outeniqua Basin [e.g., *McMillan et al.*, 1997]. Uppermost crustal velocities of between 4.5 and 5.5 km/s (Figure 6b) fit well in the velocity range of the lithologically diverse Cape Supergroup mostly consisting of sedimentary and metamorphically overprinted sedimentary rocks.

[16] The region between 300 and 350 km profile distance (Figure 6b) is characterized by the Moho's ascent from 25 to 14 km over a distance of 50 km, and an average crustal velocity of 6.07 km/s. The changes in crustal thickness and average crustal velocity across this zone classify it as a continent-ocean transition (COT) zone. Unfortunately, this part of the model is not as well resolved as the remainder, with higher uncertainties in the velocity structure and geometry. The subparallel western profile (Figure 6c) displays a COT with a similar geometry but which is better constrained [*Parsiegla et al.*, 2007], suggesting that the COT in the eastern profile is reasonable. The maximum width of this COT (50 km) fits within the known range from other sheared margin COTs (50–80 km [*Bird*, 2001]).

[17] The crustal thickness in the Agulhas Passage varies between 6 and 10 km (350 to 435 km profile distance). Although this thickness is in the normal range for oceanic crust, the average (crystalline) crustal velocity of 6.04 km/s is at the lower limit of those reported [*Mutter and Mutter*, 1993; *White et al.*, 1992]. Oceanic crust near fracture zones can be up to 50% thinner than normal, usually shows low average crustal velocities, and often lacks a normal oceanic layer 3 [*White et al.*, 1984, 1992]. *White et al.* [1984] attribute the observed characteristics at fracture zones to modified intrusive/extrusive processes near the transform and report evidence for serpentinization. *Sage et al.* [1997] discussed thermal effects of the adjacent continent on crustal formation processes as an explanation for the anomalously thin heterogeneous oceanic crust at the Ivory Coast–Ghana transform margin. Similar processes could provide an explanation for the relatively low average crustal velocities south of the Agulhas-Falkland Fracture Zone. In contrast to the Ivory Coast margin, we do not observe anomalously thin oceanic crust. Having the unique setting of the Agulhas Plateau Large Igneous Province being situated south of the sheared margin, it is possible that the oceanic crust in the Agulhas Passage was originally thinner than it is today and was overprinted during the formation of the plateau, e.g., by volcanic flows migrating north of the Agulhas Plateau.

[18] On the Agulhas Plateau (profile distance 435–890 km), the crustal thickness increases again to an average of 20 km, with an average crustal velocity of 6.5 km/s. This significantly higher average crustal velocity is due to the Agulhas Plateau's ~10 km thick high-velocity lower crustal body, which identifies it as a Large Igneous Province [*Parsiegla et al.*, 2008].

5. Crustal Stretching and Tectonic Processes Along/Across the Southern African Margin

5.1. Calculation of Crustal Stretching Factors

[19] On the basis of our crustal velocity-depth models north of 150 km profile distance, where very little or no crustal stretching is expected (Figures 6b and 6c), we assume initial crustal thicknesses before stretching, *Tc*, of 43 km for the western profile and 42 km for the eastern profile. The continental crust thins between distances 180 and 520 km on the western profile, most

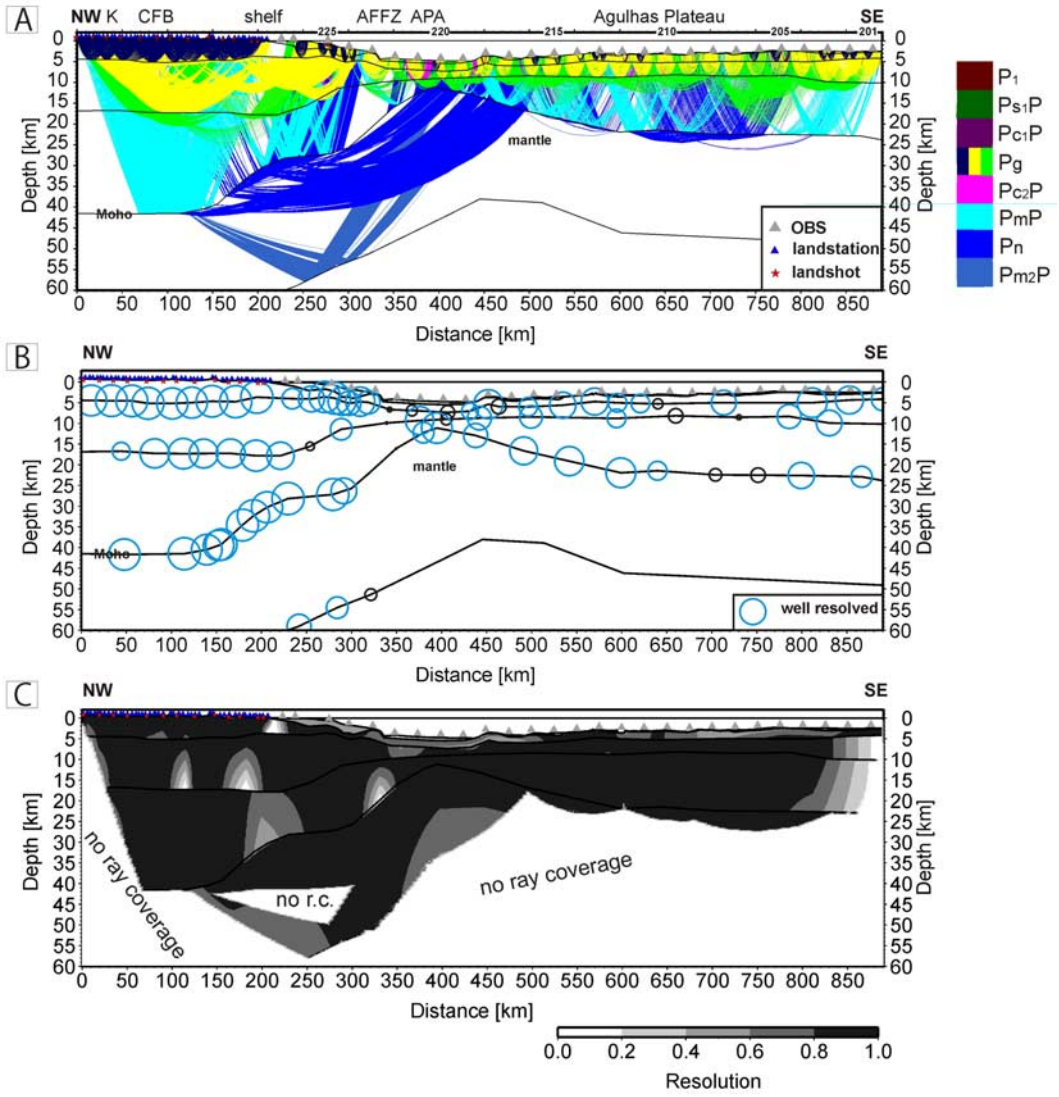

Figure 7. Quality control of the eastern profile (AWI-20050200-GRA). Abbreviations are as follows: AFFZ, Agulhas-Falkland Fracture Zone; APA, Agulhas Passage; CFB, Cape Fold Belt; K, Karoo. (a) Plot of the ray coverage with rays modeling reflected and refracted waves. Different colors represent different phases where the assignment of the colors to the phases (see also Table 2) can be found in the legend on the right. (b) Resolution of depth nodes of the velocity-depth model. Blue circles represent a good resolution. Black circles mark depth nodes with a resolution of less than 0.5. The circle diameter corresponds to the resolution, where circles with the largest diameter have a resolution of 0.95. For the bottom of the first layer, 75% of the depth nodes in the offshore part of the profile are well resolved (layer one does not exist onshore), but the nodes are too numerous to be clearly arranged and are therefore not displayed.

likely because of crustal stretching (Figure 6c). A significantly smaller part of the eastern profile consists of stretched continental crust (Figures 6a and 6b, 150–340 km profile distance). For both profiles, we measured the (crystalline) crustal thickness, *Ts*, of these stretched regions at 10 km intervals and calculated the stretching factors $\beta = Tc/Ts$ (Figure 8).

[20] Stretching factors increase from north to south along both profiles (Figure 8). The lowest stretching factors were observed in the southernmost CFB with average β factors of 1.1–1.2. Peak β factors occur next to the AFFZ (β = 3.2–3.3). Stretching factors in the Pletmos and Gamtoos Basins are similar (β = 1.6), while in the Southern Outeniqua Basin β = 1.9.

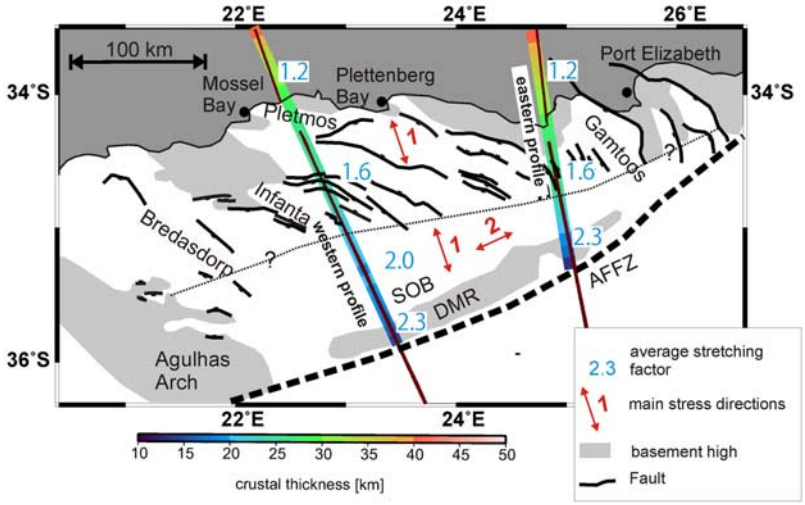

Figure 8. Outeniqua Basin with color-coded crystalline crustal thickness along the profiles and average stretching factors. The subdivision between the area of the Outeniqua Basin which experienced one and the area which was affected by two stretching episodes is marked by a dashed line. The approximate stress directions are shown as red arrows. Arrow 1 shows the direction in Jurassic times, and arrow 2 shows the direction in Cretaceous times. The locations of the main faults and basement highs are adapted from *South African Agency for Promotion of Petroleum Exploration and Exploitation* [2003].

5.2. Discussion of the Observed Stretching Factors, Their Possible Implications, and Tectonic Processes Along/Across the Margin

[21] With a discussion of extension geometries in pure and simple shear regimes, *Jackson* [1987] showed that the accommodation of stretching factors of more than 1.7 is most likely to require more than one set of faults. Thus, the clear step in our calculated Outeniqua Basin stretching factors can be interpreted as reflecting one episode of extension in the northern subbasins and two episodes in the wider southern basin. Furthermore, it is most economical to assume that one of these episodes affected both the northern and southern basins to achieve a stretching factor of 1.6 (Figure 8). To account for the additional stretching in the southern Outeniqua Basin, a β factor of 1.3 has to be added.

[22] Earlier studies based on seismic reflection and well data showed that rifting in the Outeniqua Basin started in middle to late Jurassic times [*Broad et al.*, 2006; *McMillan et al.*, 1997]. *McMillan et al.* [1997] suggested that this rifting accompanied the breakup between East Gondwana (Antarctica, Australia, India) and West Gondwana (South America, Africa) that eventually gave rise seafloor spreading in the Riiser Larsen and Weddell seas (Figures 8 and 9) [e.g., *Eagles and König*, 2008; *Jokat et al.*, 2003; *König and Jokat*, 2006]. From our stretching factors, we infer that this episode resulted in crustal thinning over the whole basin (Figure 8) and up to ~50 km inland of the present-day coast. The second episode probably accompanied shear motion along the active Agulhas-Falkland transform system, i.e., in early Cretaceous times when the stress direction was subparallel to the present-day AFFZ at ~136 Ma (Figures 8 and 9). Consistent with this, seismic reflection and well data exhibit an upper Valanginian unconformity (~135 Ma) [*Broad et al.*, 2006; *McMillan et al.*, 1997] and *McMillan et al.* [1997] report evidence for strike-slip faulting in the southern Outeniqua Basin.

[23] The Diaz Marginal Ridge (DMR) forms the southern boundary of the Southern Outeniqua Basin. Suggestions for the time of its formation range from before the first shear motion along the AFFZ [*Ben-Avraham et al.*, 1997] to contemporaneous with it [*McMillan et al.*, 1997]. Results from our seismic reflection measurements show that the DMR is buried by 200–250 m of sediments and sedimentary rocks (Figure 4). Assuming the stratigraphy of the northern parts of the Outeniqua Basin [*Broad et al.*, 2006] can be extrapolated onto the DMR, we observe 150 to 200 m of undisturbed Cretaceous sedimentary cover over the DMR (Figure 4). These rocks are younger than the oldest Cretaceous sedimentary rocks in the Southern Outeniqua Basin (Figure 4). This in turn, places the formation time of the DMR after the initial movement along the Agulhas Falkland Transform. As

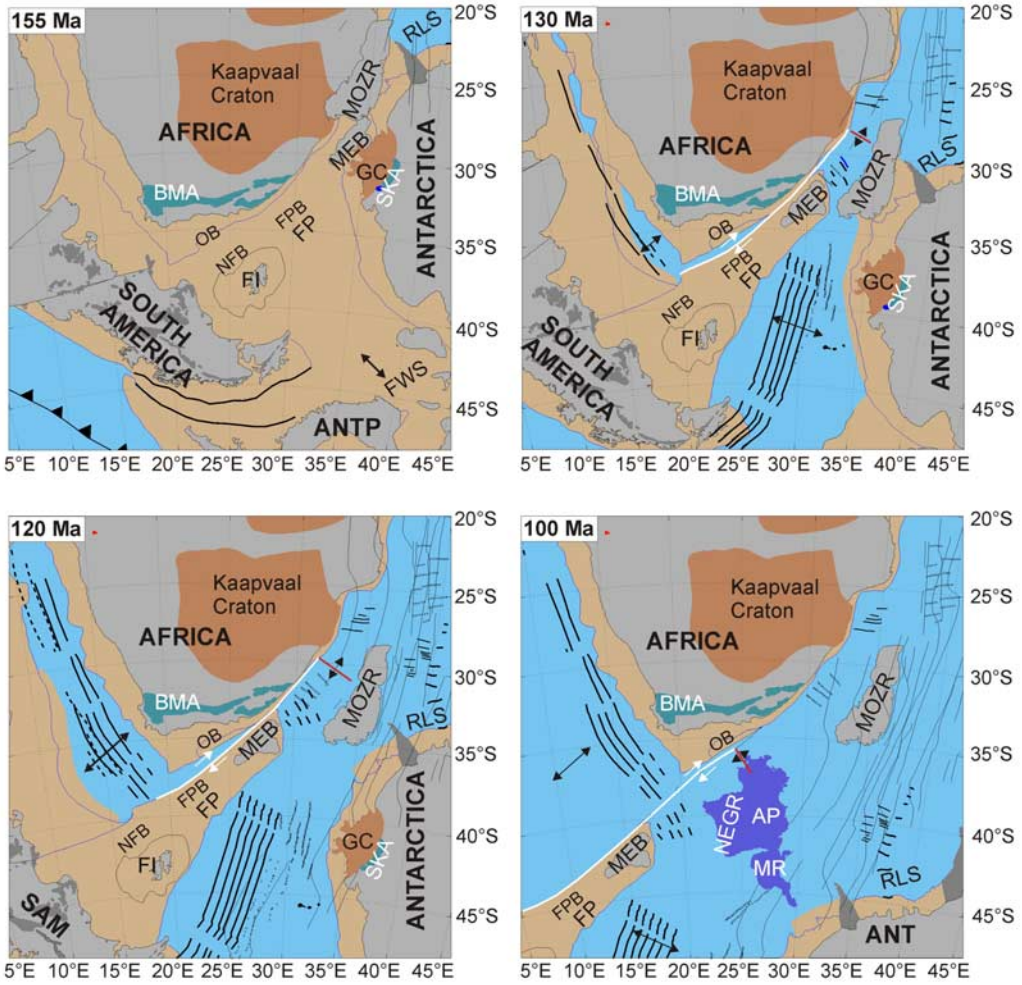

Figure 9. Plate tectonic reconstruction for the main steps of the southern African margin evolution using the rotation poles of *König and Jokat* [2006]. We use the present-day coordinate system for orientation. The rotations were performed with respect to Africa. Before 155 Ma, Africa and South America are still attached to each other. The Gondwana breakup between Africa and Antarctica and the related stress field had possibly caused the onset of the rifting episode in the Outeniqua Basin (OB) and in the sedimentary basins of the Falkland Plateau (FP). At 130 Ma, seafloor spreading takes place in the Weddell Sea, Riiser Larsen Sea (RLS), north of the Maurice Ewing Bank (MEB), and has started in the South Atlantic. Note the position of the spreading ridge northeast of the MEB (red). The shear motion along the Agulhas Falkland Transform started ~136 Ma and actively forms the continental margin in this early drift stage and caused a second pulse of crustal stretching in the Outeniqua Basin. At 120 Ma, in the later drift stage, transtension along the AFT is still responsible for crustal thinning in the southern parts of the Outeniqua Basin and the Falkland Plateau Basin (FPB). At 100 Ma, the Agulhas Plateau (AP) developed together with Maud Rise (MR) and Northeast Georgia Rise (NEGR). The thermal conditions along the margin have changed as hot young oceanic crust slides along old continental crust with the spreading ridge (red) perpendicular to the Outeniqua Basin. ANTP, Antarctic Peninsula; BMA, Beattie magnetic anomaly; FWS, future Weddell Sea; GC, Grunehogna Craton; MOZR, Mozambique Ridge; NFB, North Falkland Basin; SKA, Sverdrupfjella-Kirvanveggen magnetic anomaly.

sedimentation and erosion rates are unknown and any drill hole control is lacking in this region, the formation time of the DMR can only be estimated within a wide time range between 130 and 90 Ma. In this time span, two formation mechanisms are discussed. One possible scenario was described by *Parsiegla et al.* [2007]. They suggest that the DMR was uplifted from a metasedimentary basin during a transpressional episode along the Agulhas-Falkland Transform. We modeled a similar crustal thickness beneath the DMR as observed beneath the Southern Outeniqua Basin (Figures 6b, 6c, and 8). Therefore, it is likely that the crust beneath the marginal ridge experienced the same extensional episodes as the Southern Outeniqua Basin. This makes a setting more likely in which the crust of

Table 4. Average Crustal Thicknesses of the Outeniqua Basin and the Falkland Plateau Basin With Standard Deviations of the Values Derived in This Study

Basin	Average Crustal Thickness (km)	Basis of Information	Reference
Outeniqua Basin (Pletmos Basin)	27 ± 2	seismic refraction profiling	this study
Outeniqua Basin (Gamtoos Basin)	26 ± 1	seismic refraction profiling	this study
Outeniqua Basin (Southern Outeniqua Basin)	21 ± 1	seismic refraction profiling	this study
Falkland Plateau Basin	19–23	3-D gravity modeling	*Kimbell and Richards* [2008]

the DMR was first stretched and then uplifted. In this second scenario, the DMR developed when newly formed oceanic crust slid past old continental crust in the continent-ocean shear stage. With this configuration of (hot) oceanic crust and (cold) continental crust opposed across the Agulhas-Falkland Transform, it is likely that a significant temperature contrast existed across the transform fault during the drift episode, especially when the spreading ridge passed. Therefore we propose that this temperature contrast could have induced a thermal uplift of the DMR. Induced thermal uplift has also been suggested for other sheared margins, e.g., the Ivory Coast–Ghana transform margin [*Basile et al.*, 1993], the Senja Fracture Zone (SW Barents Sea [*Vågnes*, 1997]), and the Demerara Plateau (French Guiana–Northeast Brazil margin [*Greenroyd et al.*, 2008]). Numerical simulations of induced thermal uplift were able to model the height, extent and shape of marginal ridges realistically [e.g., *Gadd and Scrutton*, 1997; *Vågnes*, 1997]. The thin continental crust beneath the DMR could be an argument against transpression as a formative mechanism. Because of the lack of drill holes into the DMR, its composition is still unknown. A metasedimentary composition is inferred from low seismic P wave velocities in the Diaz Marginal Ridge [*Parsiegla et al.*, 2007] and evidence that Cape Supergroup rocks underlie parts of the Outeniqua Basin [*McMillan et al.*, 1997]. Such a composition is consistent with that of the Ivory Coast marginal ridge, the only marginal ridge which was drilled so far [*Mascle et al.*, 1997].

5.3. Comparison Between Crustal Stretching and Formation of the Outeniqua and Falkland Basins

[24] During the rifting period (Figure 9) of the sheared margin the future Outeniqua Basin was situated opposite the Falkland Plateau [e.g., *Martin et al.*, 1981, 1982]. Knowledge of the development of the plateau is complicated by the proposed rotation of a Falkland Islands plate [e.g., *Adie*, 1952; *Storey et al.*, 1999] that dates from 178 to 121 Ma [*Stone et al.*, 2008] that may or may not have accompanied extension in its sedimentary basins. Recent plate tectonic reconstructions that use movements on a Gastre Fault system show the Outeniqua Basin contiguous with the North Falkland Basin [*Jokat et al.*, 2003; *König and Jokat*, 2006] (Figure 9). The rift stage in the North Falkland Basin is constrained to mid-Jurassic times, albeit not tightly [*Richards and Hillier*, 2000] (Figure 2), and *McMillan et al.* [1997] suggested the possible presence of pre-Kimmeridgian sedimentary rocks (>155 Ma) in the Outeniqua Basin. While this is not inconsistent with recent reconstructions, *von Gosen and Loske*'s [2004] field-based study of the Gastre Fault reported no evidence for dextral shear, but for downfaulting. Plate tectonic reconstructions, which do not incorporate shear motion along the Gastre Fault, showed the Falkland Plateau Basin as a southern extension of the Outeniqua Basin [*Eagles*, 2007; *Martin et al.*, 1982]. This seems to be supported by dating of the oldest sedimentary rocks at Deep Sea Drilling Project (DSDP) sites 327A (leg 36), 330 (leg 36) and 511 (leg 71) on the eastern flank of the Falkland Plateau (Figure 2) to Kimmeridgian/Oxfordian times [*Jeletzky*, 1983; *Jones and Plafker*, 1977]. As neither the DSDP sites, nor the drill holes in the Outeniqua Basin sampled the oldest rift sedimentary rocks in the basins, it is very likely that rifting in these basins started already in mid-Jurassic times.

[25] Recent 3-D gravity modeling on the Falkland Plateau revealed a crustal thickness of between 19 and 23 km on the Falkland Plateau Basin [*Kimbell and Richards*, 2008], a range that includes our determination of the crustal thickness beneath the Southern Outeniqua Basin (~21 km; Table 4). If we take the same initial crustal thickness of 43 km

Table 5. Summary of the Development of the Southern African Continental Margin From Initiation of Basin Formation to the Present-Day Postshear Stage

Time	Event
~169–155 Ma	first rifting started to form the Outeniqua and Falkland Plateau Basins
From ~136 Ma	start of shear motion along the Agulhas-Falkland Transform
	further crustal stretching in the southern parts of the Outeniqua Basin and the Falkland Plateau Basin
	continent-continent shear stage of the transform margin
~130–90 Ma	formation of the Diaz Marginal Ridge either due to transpression or thermal uplift (in a short episode within this interval)
~115–84 Ma	continent-ocean shear stage
~100–94 Ma	formation of the Agulhas Plateau Large Igneous Province
	uplift of southern Africa
	increased denundation onshore
From ~84 Ma	postshear stage
~64–58 Ma	two ridge jumps reduced the ridge-ridge offset of the Agulhas-Falkland Transform to its present offset of ~290 km

as proposed for the Outeniqua Basin, it is not surprising that these thicknesses imply stretching factors of between 1.9 and 2.3, similar to those that we have calculated for the Southern Outeniqua Basin (1.8–2.1). Hence, it seems likely that the Falkland Plateau Basin experienced the same two extensional episodes as the southern extent of the Outeniqua Basin.

6. Evolution of the Margin

[26] Rifting started to form the Outeniqua and Falkland Plateau Basins in mid-late Jurassic times (Figure 9). Shear motion along the Agulhas-Falkland Transform can be considered as the cause of additional stretching in the southern parts of the Outeniqua Basin in early Cretaceous times (Figure 9). These two episodes formed a large basin during the breakup of Gondwana and through the early continent-continent shear stage of West Gondwana breakup (Figure 9 and Table 5).

[27] Most important for the evolution of the southern African margin from ~136 Ma onward was the development of the Agulhas-Falkland Transform Fault (and later its remnant structure, the AFFZ). It is not clear whether this transform developed entirely in the Cretaceous [e.g., *Broad et al.*, 2006] or represents the reactivation of a preexisting crustal feature [e.g., *Jacobs and Thomas*, 2004]. Our data and drill hole evidence [*McMillan et al.*, 1997] suggest that the CFB underlies the Outeniqua Basin, raising the question of whether the transform is a reactivated Gondwanide orogenic structure. *Johnston* [2000] showed a model for the formation of the CFB during dextral transpressional processes suggesting that structures suitable for reactivation in a strike-slip mode existed in this region well before early Cretaceous times. However, the azimuths of Johnston's proposed structures are not consistent with the development of an NE–SW directed shear along the intracontinental Agulhas-Falkland Transform about 100 Ma later. If a preexisting structure is to be invoked, then, it may be that one has to look back to before the Gondwanide orogeny. *Jacobs and Thomas* [2004] suggested that shear zones may have developed in the region during lateral escape tectonics related to the East African–Antarctic orogen. Another possibility is the reactivation of an old trench-linked strike-slip fault as a very deep seated fault type with high preservation and reactivation potential [*Woodcock*, 1986].

[28] But why was such a large-scale transform possible in the first place? We have already looked at the possibility of zones of lithospheric weakness formed during southern Africa's billions of years history of continental accretion and dispersal. Additionally, the sites of original breakup may have been influenced by the presence and action of plumes (e.g., that forming the Karoo Large Igneous Province [e.g., *Duncan et al.*, 1997; *Ernst and Buchan*, 2002]). Plume activity possibly weakened the lithosphere enough for the reactivation of preexisting faults into an intracontinental, and later ridge-offset, transform (Figure 9).

[29] The formation of the Diaz Marginal Ridge can be tentatively dated to between 130 and 90 Ma (this study). Either a transpressional episode along the Agulhas-Falkland Transform or a temperature difference across the transform (Figure 9) caused its uplift.

[30] At about 100 Ma the spreading ridge was approximately located at the western margin of the present-day Agulhas Plateau. This oceanic plateau has been identified as a Large Igneous Province (LIP) [*Gohl and Uenzelmann-Neben*, 2001; *Uenzelmann-Neben et al.*, 1999] (Figure 9). The development of this LIP can be related to the location of the Bouvet triple junction on its southwestern edge and the activity of the Bouvet

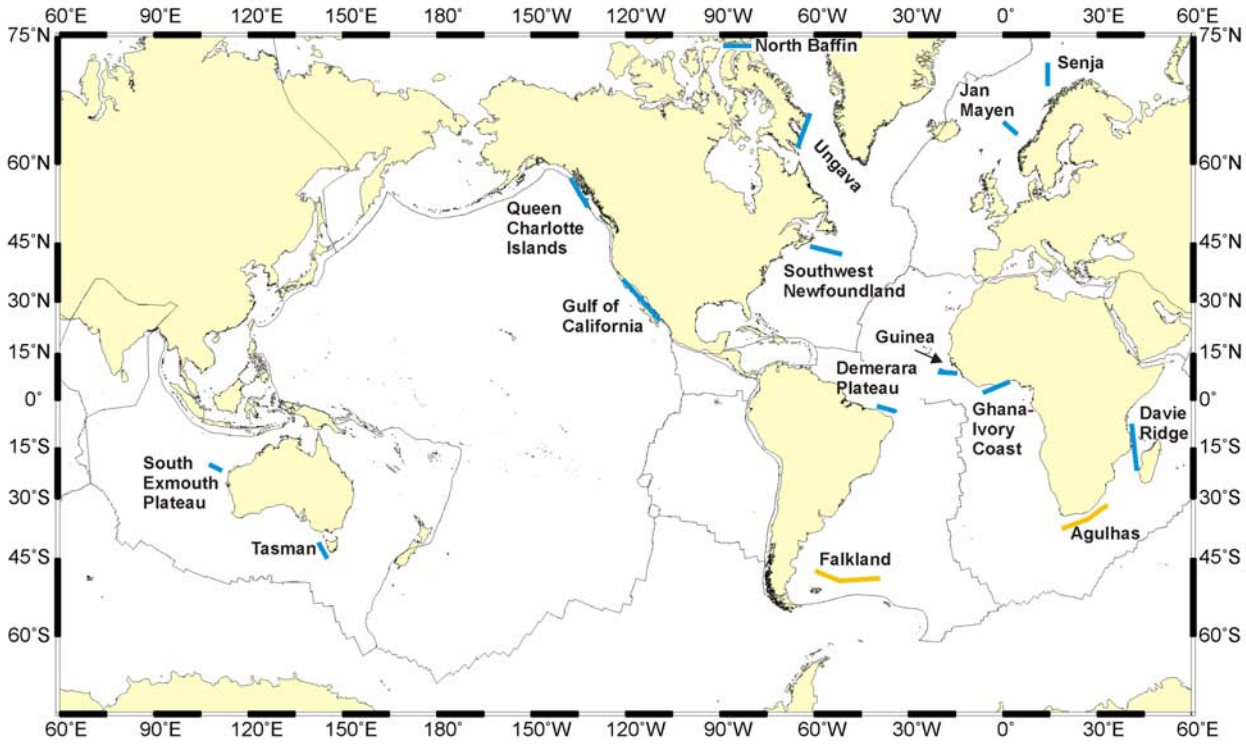

Figure 10. Compilation of the major transform margins (blue). The transform margins bounded by the Agulhas-Falkland Fracture Zone are highlighted in orange. The positions of the sheared margins are from *Lorenzo* [1997] and *Greenroyd et al.* [2008].

plume [*Parsiegla et al.*, 2008]. During the ~6 Ma formation time [*Parsiegla et al.*, 2008] this massive volcanism had a great impact on crustal generation south of and possibly in the Agulhas Passage. Contemporaneous uplift of southern Africa (100–80 Ma [e.g., *Tinker et al.*, 2008]) and the injection of kimberlites (108–74 Ma [e.g., *Kobussen et al.*, 2008]) can be interpreted as indications that these mantle processes had an influence even further north.

[31] The beginning of the postshear phase of the margin, the present state of the southern African continental margin, can be estimated at ~84 Ma. From this time onward active parts of Agulhas-Falkland Fracture Zone system (i.e., the transform itself) where not longer opposite the African continent but had moved to the west. Spreading ridge jumps in the South Atlantic at about 61–64 Ma [*Barker*, 1979; *Marks and Stock*, 2001] and 60–58 Ma [*Barker*, 1979] caused a significant reduction of the transform offset and led to its present ridge-ridge offset of about 290 km. Neotectonic activity at the Agulhas-Falkland Fracture Zone was identified [*Ben-Avraham*, 1995; *Parsiegla et al.*, 2007] and may be an expression of lithospheric weakness along the Agulhas-Falkland Fracture Zone acting to accommodate the uplift of southern Africa.

7. Comparison With Other Transform Margins

[32] Observations from other transform margins have shown that deep sedimentary basin on their continental side, followed by a marginal ridge and the continent-ocean fracture zone, is characteristic [*Lorenzo*, 1997]. This is consistent with our observations from the southern African margin. Comparing the various sheared margins in the world (Figure 10), structures of sheared margins are more miscellaneous. The structures found at a transform margin depend on the stage of its development.

[33] An example of a margin in the active continent-ocean shear phase is found at the Queen Charlotte margin in western Canada (Figure 10). At this margin, a significant component of convergence has occurred in addition to the strike-slip process. This transpressional regime causes underthrusting of the Pacific Plate beneath the North American Plate [*Prims et al.*, 1997]. The accretion of marine sediments led to the development a

sedimentary wedge (the Queen Charlotte Terrace) on the Pacific Plate, and the Queen Charlotte Trough formed because of the load onto the North American Plate [*Prims et al.*, 1997]. In contrast to the common characteristics of sheared margins described by *Lorenzo* [1997], no uplifted marginal ridge is found here, but uplift influenced the continental side of the margin by forming the Queen Charlotte Islands. The sedimentary wedge at this margin is not common at other sheared margins. The deep basin is a result of flexure instead of rifting as observed for the Outeniqua Basin of the southern African margin.

[34] The southwest Newfoundland margin is another example of a unique transform margin because oceanic crust overlays thinned continental crust for the parts of the margin investigated by *Todd et al.* [1988]. In spite of this complexity, *Todd and Keen* [1989] modeled the thermal uplift as a result of lateral conduction from oceanic to continental lithosphere along the Newfoundland margin. They found that frictional heating due to shear processes only plays a secondary role in this scenario. The zone of uplift at the Newfoundland margin (60–80 km [*Todd and Keen*, 1989]) is broader than at other sheared margins such as the Exmouth Plateau (~30 km) and the southern African margin (~40 km). In general, the uplift is most likely restricted to a region of <100 km distance from the continent-ocean transform. Transpression as uplift mechanism is only observed at a few transform margins, e.g., the Queen Charlotte margin, while conduction (with or without flexural coupling between continental and oceanic lithosphere) can be considered as the major driving mechanism for uplift at the continental side of a continent-ocean transform, e.g., the south Newfoundland [*Todd and Keen*, 1989], the Ivory Coast [*Basile et al.*, 1993] and the northern Falkland [*Lorenzo and Wessel*, 1997] margins.

[35] In the case of the southern African margin, this discussion sheds more light on the mechanism that formed the Diaz Marginal Ridge. This study shows that the formation time of the ridge makes thermal uplift (i.e., heat conduction) and transpressional scenarios possible. A comparison with the typical features of a strongly transpressional margin, the Queen Charlotte margin, with underthrusting and a thick sedimentary wedge on the oceanic side of the margin shows that the lack of such characteristics at the southern African margin is an indicator that the influence of conduction exceeds transpression. The thin crust beneath the Diaz Marginal Ridge and the observed P wave velocities, indicating slight metamorphosis, are further arguments against the domination of a transpression mechanism.

8. Conclusions

[36] Two combined land-sea velocity-depth models, derived from seismic refraction/wide-angle reflection data of the Agulhas-Karoo Geoscience Transect, and seismic reflection data were presented in this study. They provide new insights into the crustal structure of southern African continental transform margin (Figure 6) and provide conclusions about the nature and timing of the related tectonic/geodynamic processes (Figure 9 and Table 1).

[37] Both profiles cross continental, stretched continental, transitional and oceanic crust. From crustal thickness information of unstretched and stretched continental crust, we calculated crustal stretching factors in the Outeniqua Basin which provide important indications to understand the basin formation. Stretching factors lower than 1.7 are interpreted to be the result of an episode of crustal extension which was attributed to the rift stage of the basin. This was possibly initiated by stresses associated with the breakup between Africa and Antarctica. This episode had influence on the whole Outeniqua Basin and the conjugate Falkland Plateau Basin. A second stretching episode, possibly related to shear motion along the Agulhas Falkland transform system starting in Valanginian times, is hinted at by stretching factors >1.7 in the southern parts of the Outeniqua Basin and Falkland Plateau Basin.

[38] The crustal velocities in the Diaz Marginal Ridge and its sedimentary cover are used to discuss two models of its formation. A transpressional episode or a temperature difference across the transform may have been responsible for the uplift of the Diaz Marginal Ridge. The hypothesis of a thermal uplift is a more likely cause because similar stretching factors in the Southern Outeniqua Basin and Diaz Marginal Ridge suggest a common stretching history. Lacking evidence of transpressional features at the southern African margin, e.g., underthrusting, constitutes another point in favor of thermal uplift.

[39] As the formation of the Agulhas-Falkland Transform is important for the margin's evolution we discussed if it is a Cretaceous feature or related to older tectonic processes. Even with our new high-quality data, the question of whether the

Agulhas-Falkland Transform exploited a preexisting zone of crustal/lithospheric weakness cannot be conclusively answered. However, supercontinent amalgamation and dispersal processes together with plume activity in this region provide scenarios which make reactivation more likely than a first formation in the Cretaceous.

Acknowledgments

[40] We acknowledge the excellent cooperation of Captain L. Mallon and the crew of R/V *Sonne* as well as the AWI geophysics team during cruise SO-182. We would like to thank the two anonymous reviewers for their helpful comments. We are grateful to Ernst Flüh of IFM-GEOMAR for lending us 40 OBS systems. The equipment of the onshore experiments was provided by the Geophysical Instrument Pool of GFZ Potsdam. We thank the seismic and MT field teams as well as the farmers who granted us access to their land. We are grateful to Graeme Eagles who greatly improved this manuscript by invaluable comments on a prereview version. We thank Jan Grobys and Anthony Tankard for valuable discussions. Thanks to Matthias König for providing access to his plate rotation code and an initial introduction. Many thanks to Maarten de Wit (UCT and Africa Earth Observatory Network) for his support before and during the research visit of N.P. in Cape Town. The German Academic Exchange Service (DAAD) funded a research visit of N.P. at the University of Cape Town (South Africa), where parts of the research were carried out. Figures 1–8 and 10 were generated using GMT software [*Wessel and Smith*, 1998]. The SO-182 cruise (project AISTEK-I) and N.P.'s Ph.D. position were primarily funded by the German Bundesministerium für Bildung und Forschung (BMBF) under contract 03G0182A. This is Inkaba ye Africa contribution 31.

References

Adie, R. J. (1952), The position of the Falkland islands in a reconstruction of Gondwanaland, *Geol. Mag.*, *89*, 401–410.

Barker, P. F. (1979), The history of ridge-crest offset at the Falkland-Agulhas Fracture Zone from a small-circle geophysical profile, *Geophys. J.R. Astron. Soc.*, *59*, 131–145.

Basile, C., J. Mascle, M. Popoff, J. P. Bouillin, and G. Mascle (1993), The Ivory Coast-Ghana transform margin: A marginal ridge structure deduced from seismic data, *Tectonophysics*, *222*, 1–19, doi:10.1016/0040-1951(93)90186-N.

Ben-Avraham, Z. (1995), Neotectonic activity offshore southeast Africa and its implications, *S. Afr. J. Geol.*, *98*, 202–207.

Ben-Avraham, Z., C. J. H. Hartnady, and J. A. Malan (1993), Early tectonic extension between the Agulhas Bank and the Falkland Plateau due to the rotation of the Lafonia microplate, *Earth Planet. Sci. Lett.*, *117*, 43–58, doi:10.1016/0012-821X(93)90116-Q.

Ben-Avraham, Z., C. J. H. Hartnady, and A. P. le Roex (1995), Neotectonic activity on continental fragments in the southwest Indian Ocean: Agulhas Plateau and Mozambique Ridge, *J. Geophys. Res.*, *100*, 6199–6211, doi:10.1029/94JB02881.

Ben-Avraham, Z., C. J. H. Hartnady, and K. A. Kitchin (1997), Structure and tectonics of the Agulhas-Falkland fracture zone, *Tectonophysics*, *282*, 83–98, doi:10.1016/S0040-1951(97)00213-8.

Bird, D. (2001), Shear margins: Continent-ocean transform and fracture zone boundaries, *Leading Edge*, *20*, 150–159, doi:10.1190/1.1438894.

Broad, D. S., E. H. A. Jungslager, I. R. McLachlan, and J. Roux (2006), Geology of the offshore Mesozoic basins, in *The Geology of South Africa*, edited by M. R. Johnson et al., pp. 553–571, Geol. Soc. of S. Afr., Pretoria.

Christensen, N. I., and W. Mooney (1995), Seismic velocity structure and composition of the continental crust: A global view, *J. Geophys. Res.*, *100*, 9761–9788, doi:10.1029/95JB00259.

Cole, D. J. (1992), Evolution and development of the Karoo Basin, in *Inversion Tectonics of the Cape Fold Belt, Karoo and Creataceous Basins of Southern Africa*, edited by M. de Wit and I. G. D. Ransome, pp. 87–99, A. A. Balkema, Rotterdam, Netherlands.

de Beer, J. H., J. S. V. van Zijl, and D. I. Gough (1982), The Southern Cape Conductivity Belt (South Africa): Its composition, origin and tectonic significance, *Tectonophysics*, *83*, 205–225, doi:10.1016/0040-1951(82)90019-1.

de Wit, M., and B. Horsfield (2006), Inkaba yeAfrica project surveys sector of Earth from core to space, *Eos Trans. AGU*, *87*, 113–117, doi:10.1029/2006EO110002.

de Wit, M. J., and J. Stankiewicz (2006), Changes in surface water supply across Africa with predicted climate change, *Science*, *311*, 1917–1921, doi:10.1126/science.1119929.

Duncan, R. A., P. R. Hooper, J. Rehacek, J. S. Marsh, and A. R. Duncan (1997), The timing and duration of the Karoo igneous event, southern Gondwana, *J. Geophys. Res.*, *102*, 18,127–18,138, doi:10.1029/97JB00972.

Eagles, G. (2007), New Angles on South Atlantic opening, *Geophys. J. Int.*, *168*, 353–361, doi:10.1111/j.1365-1246X.2006.03206.x.

Eagles, G., and M. König (2008), A model of plate kinematics in Gondwana breakup, *Geophys. J. Int.*, *173*, 703–717, doi:10.1111/j.1365-1246X.2008.03753.x.

Ernst, R. E., and K. L. Buchan (2002), Maximum size and distribution in time and space of mantle plumes: Evidence from large igneous provinces, *J. Geodyn.*, *34*, 309–342, doi:10.1016/S0264-3707(02)00025-X.

Furlong, K. P., and W. D. Hugo (1989), Geometry and evolution of the San Andreas Fault Zone in northern California, *J. Geophys. Res.*, *94*, 3100–3110, doi:10.1029/JB094iB03p03100.

Gadd, S. A., and R. A. Scrutton (1997), An integrated thermomechanical model for transform continental margin evolution, *Geo Mar. Lett.*, *17*, 21–30, doi:10.1007/PL00007203.

Gohl, K., and G. Uenzelmann-Neben (2001), The crustal role of the Agulhas Plateau, southwest Indian Ocean: Evidence from seismic profiling, *Geophys. J. Int.*, *144*, 632–646, doi:10.1046/j.1365-246x.2001.01368.x.

Greenroyd, C. J., C. Pierce, M. Rodger, A. B. Watts, and R. W. Hobbs (2008), Demerara Plateau-The structure and evolution of a transform passive margin, *Geophys. J. Int.*, *172*, 549–564.

Hälbich, I. W. (1993), *The Cape Fold Belt-Agulhas Bank Transect: Across Gondwana Suture, Southern Africa*, *Global Geosci. Transect*, 9, 18 pp., AGU, Washington, D. C.

Hälbich, I. W., F. J. Fitch, and J. A. Miller (1983), Dating the Cape orogeny, *Geol. Soc. S. Afr. Spec. Publ.*, *12*, 149–164.

Hartnady, C. J. H., and A. P. le Roex (1985), Southern Ocean hotspot tracks and the Cenozoic absolute motion of the Afri-

can, Antarctic, and South American plates, *Earth Planet. Sci. Lett.*, *75*, 245–257, doi:10.1016/0012-821X(85)90106-2.

Hawkesworth, C., S. Kelly, S. Turner, A. Le Roex, and B. Storey (1999), Mantle processes during Gondwana break-up and dispersal, *J. Afr. Earth Sci.*, *28*, 239–261, doi:10.1016/S0899-5362(99)00026-3.

Jackson, J. A. (1987), Active normal faulting and crustal extension, *Geol. Soc. Spec. Publ.*, *28*, 3–17, doi:10.1144/GSL.SP.1987.1028.1101.1102.

Jacobs, J., and R. J. Thomas (2004), Himalayan-type of indenter-escape tectonics model for the southern part of the late Neoproterozoic-early Paleozoic East African-Antarctic orogen, *Geology*, *32*, 721–724, doi:10.1130/G20516.1.

Jeletzky, J. A. (1983), Macroinvertebrate palaeoontology, biochronology and palaeoenvironments of Lower Cretaceous and Upper Jurrasic rocks, Deep Sea Drilling Hole 511, Eastern Falkland Plateau, *Initial Rep. Deep Sea Drill. Proj.*, *71*, 951–975.

Johnston, S. T. (2000), The Cape Fold Belt and Syntaxis and the rotated Falkland Islands: Dextral transpressional tectonics along the southwest margin of Gondwana, *J. Afr. Earth Sci.*, *31*, 51–63, doi:10.1016/S0899-5362(00)00072-5.

Jokat, W., T. Boebel, M. König, and U. Meyer (2003), Timing and geometry of early Gondwana breakup, *J. Geophys. Res.*, *108*(B9), 2428, doi:10.1029/2002JB001802.

Jones, D. L., and G. Plafker (1977), Mesozoic megafossils from DSDP Hole 327A and Site 330 on the Eastern Falkland Plateau, *Initial Rep. Deep Sea Drill. Proj.*, *36*, 845–856.

Kimbell, G. S., and P. C. Richards (2008), The three-dimensional lithospheric structure of the Falkland Plateau region based on gravity modelling, *J. Geol. Soc.*, *165*, 795–806, doi:10.1144/0016-76492007-114.

Kobussen, A. F., W. L. Griffin, S. Y. O'Reilly, and S. R. Shee (2008), Ghosts of lithospheres past: Imaging an evolving lithosphere mantle in southern Africa, *Geology*, *36*, 515–518, doi:10.1130/G24868A.1.

König, M., and W. Jokat (2006), The Mesozoic breakup of the Weddell Sea, *J. Geophys. Res.*, *111*, B12102, doi:10.1029/2005JB004035.

Lock, B. E. (1980), Flat-plate subduction and the Cape Fold Belt of South Africa, *Geology*, *8*, 35–39, doi:10.1130/0091-7613(1980)8<35:FSATCF>2.0.CO;2.

Lorenzo, J. M. (1997), Sheared continent-ocean margins: An overview, *Geo Mar. Lett.*, *17*, 1–3, doi:10.1007/PL00007201.

Lorenzo, J. M., and P. Wessel (1997), Flexure across a continent-ocean fracture zone: Northern Falkland/Malvinas Plateau, South Atlantic, *Geo Mar. Lett.*, *17*, 110–118, doi:10.1007/s003670050015.

Marks, K. M., and J. M. Stock (2001), Evolution of the Malvinas Plate south of Africa, *Mar. Geophys. Res.*, *22*, 289–302, doi:10.1023/A:1014638325616.

Martin, A. K. (1987), Plate reorganisations around Southern Africa, hot spots and extinctions, *Tectonophysics*, *142*, 309–316, doi:10.1016/0040-1951(87)90129-6.

Martin, A. K., C. J. H. Hartnady, and S. W. Goodland (1981), A revised fit of South America and south central Africa, *Earth Planet. Sci. Lett.*, *75*, 293–305.

Martin, A. K., S. W. Goodlad, C. J. H. Hartnady, and A. du Plessis (1982), Cretaceous palaeopositions of the Falkland Plateau relative to southern Africa using Mesozoic seafloor spreading anomalies, *Geophys. J.R. Astron. Soc.*, *71*, 567–579.

Mascle, J., P. Lohmann, and P. Clift (1997), Development of a passive transform margin: Côte d'Ivoire-Ghana transform margin-ODP Leg 159 preliminary results, *Geo Mar. Lett.*, *17*, 4–11, doi:10.1007/PL00007205.

McMillan, I. K., G. I. Brink, D. S. Broad, and J. J. Maier (1997), Late Mesozoic basins off the south coast of South Africa, in *African Basins*, edited by R. C. Selley, pp. 319–376, Elsevier, Amsterdam.

Mutter, C. Z., and J. C. Mutter (1993), Variations in thickness of layer 3 dominate oceanic crustal structure, *Earth Planet. Sci. Lett.*, *117*, 295–317, doi:10.1016/0012-821X(93)90134-U.

Pankhurst, R. J., C. W. Rapela, C. M. Fanning, and M. Márquez (2006), Gondwanide continental collision and the origin of Patagonia, *Earth Sci. Rev.*, *76*, 235–257, doi:10.1016/j.earscirev.2006.02.001.

Parsiegla, N., K. Gohl, and G. Uenzelmann-Neben (2007), Deep crustal structure of the sheared South African continental margin: First results of the Agulhas-Karoo Geoscience Transect, *S. Afr. J. Geol.*, *110*, 393–406, doi:10.2113/gssajg.110.2-3.393.

Parsiegla, N., K. Gohl, and G. Uenzelmann-Neben (2008), The Agulhas Plateau: Structure and evolution of a large igneous province, *Geophys. J. Int.*, *174*, 336–350, doi:10.1111.j.1365-1246X.2008.03808.x.

Pe'eri, S., S. Wdowinski, A. Shtibelman, and N. Bechor (2002), Current plate motion across the Dead Sea Fault from three years of continuous GPS monitoring, *Geophys. Res. Lett.*, *29*(14), 1697, doi:10.1029/2001GL013879.

Prims, J., K. P. Furlong, K. M. M. Rohr, and R. Govers (1997), Lithospheric structure along the Queen Charlotte margin in western Canada: Constraints from flexural modeling, *Geo Mar. Lett.*, *17*, 94–99, doi:10.1007/s003670050013.

Richards, P. C., and B. V. Hillier (2000), Post-drilling analysis of the North Falkland Basin-Part 1: Tectono-stratigraphic framework, *J. Pet. Geol.*, *23*, 253–272.

Sage, F., B. Pontoise, J. Mascle, and C. Basile (1997), Structure of oceanic crust adjacent to a transform margin segment: The Côte d'Ivoire-Ghana transform margin, *Geo Mar. Lett.*, *17*, 31–39.

Scrutton, R. A. (1976), Crustal structure at the continental margin south of South Africa, *Geophys. J.R. Astron. Soc.*, *44*, 601–623.

Scrutton, R. A. (1979), On sheared passive continental margins, *Tectonophysics*, *59*, 293–305, doi:10.1016/0040-1951(79)90051-9.

Smith, W. H. F., and D. T. Sandwell (1997), Global seafloor topography from satellite altimetry and ship depth soundings, *Science*, *277*, 1957–1962.

South African Agency for Promotion of Petroleum Exploration and Exploitation (2003), South African exploration opportunities, Parow, Cape Town.

Stankiewicz, J., T. Ryberg, A. Schulze, A. Lindeque, M. H. Weber, and M. J. de Wit (2007), Results from wide-angle seismic refraction lines in the southern Cape, *S. Afr. J. Geol.*, *110*, 407–418, doi:10.2113/gssajg.110.2-3.407.

Stankiewicz, J., N. Parsiegla, T. Ryberg, K. Gohl, U. Weckmann, R. Trumbull, and M. Weber (2008), Crustal structure of the southern margin of the African continent: Results from geophysical experiments, *J. Geophys. Res.*, *113*, B10313, doi:10.1029/2008JB005612.

Stone, P., P. C. Richards, G. S. Kimbell, R. P. Esser, and D. Reeves (2008), Cretaceous dykes discovered in the Falkland Islands: Implications for regional tectonics in the South Atlantic, *J. Geol. Soc.*, *165*, 1–4, doi:10.1144/0016-76492007-072.

Storey, B. C., M. L. Curtis, J. K. Ferris, M. A. Hunter, and R. A. Livermore (1999), Reconstruction and break-out model for the Falkland Islands within Gondwana, *J. Afr. Earth Sci.*, *29*, 153–163, doi:10.1016/S0899-5362(99)00086-X.

Tankard, A. J., M. P. A. Jackson, K. A. Eriksson, D. K. Hobday, D. R. Hunter, and W. E. L. Minter (1982), *Crustal Evolution of Southern Africa*, 523 pp., Springer, New York.

Thomson, K. (1999), Role of the continental break-up, mantle plume development and fault activation in the evolution of the Gamtoos Basin, South Africa, *Mar. Pet. Geol.*, *16*, 409–429, doi:10.1016/S0264-8172(99)00010-0.

Tinker, J., M. de Wit, and R. Brown (2008), Mesozoic exhumation of the southern Cape, South Africa, quantified using apatite fission track thermochronology, *Tectonophysics*, *455*, 77–93, doi:10.1016/j.tecto.2007.10.009.

Todd, B. J., and C. E. Keen (1989), Temperature effects and their geological consequences of transform margins, *Can. J. Earth Sci.*, *26*, 2591–2603, doi:10.1139/e89-221.

Todd, B. J., I. D. Reid, and C. E. Keen (1988), Crustal structure across the southwest Newfoundland transform margin, *Can. J. Earth Sci.*, *25*, 744–759.

Uenzelmann-Neben, G., (Ed.) (2005), Southeastern Atlantic and southwestern Indian Ocean: Reconstruction of the sedimentary and tectonic development since the Cretaceous-AISTEK–I: Agulhas Transect, Report on RV *Sonne* cruise SO–182, *Rep. on Polar and Mar. Res., 515*, 73 pp., Alfred Wegener Inst. for Polar and Mar. Res., Bremerhaven, Germany.

Uenzelmann–Neben, G., K. Gohl, A. Ehrhardt, and M. Seargent (1999), Agulhas Plateau, SW Indian Ocean: New evidence for excessive volcanism, *Geophys. Res. Lett.*, *26*, 1941–1944, doi:10.1029/1999GL900391.

Vågnes, E. (1997), Uplift at thermo–mechanical coupled ocean–continent transforms: Modeled at the Senja Fracture Zone, southwestern Barents Sea, *Geo Mar. Lett.*, *17*, 100–109, doi:10.1007/s003670050014.

Vaughan, A. P. M., and R. J. Pankhurst (2008), Tectonic overview of the West Gondwana margin, *Gondwana*, *13*, 150–162, doi:10.1016/j.gr.2007.07.004.

von Gosen, W., and W. Loske (2004), Tectonic history of the Calcatapul Formation, Chubut province, Argentina, and the "Gastre fault system,", *J. South Am. Earth Sci.*, *18*, 73–88, doi:10.1016/j.jsames.2004.08.007.

Wessel, P., and W. H. F. Smith (1998), New, improved version of generic mapping tools released, *Eos Trans. AGU*, *79*, 579, doi:10.1029/98EO00426.

White, R. S., and D. McKenzie (1992), Oceanic crustal thickness from seismic measurements and rare earth element inversions, *J. Geophys. Res.*, *97*, 19,683–19,715, doi:10.1029/92JB01749.

White, R. S., R. S. Detrick, M. C. Sinha, and M. H. Cormier (1984), Anomalous seismic crustal structure of oceanic fracture zones, *Geophys. J. R. Astron. Soc.*, *79*, 779–798.

Woodcock, N. H. (1986), The role of strike–slip fault systems at plate boundaries, *Philos. Trans. R. Soc. London, Ser. A*, *317*, 13–29, doi:10.1098/rsta.1986.0021.

Zelt, C. A., and R. B. Smith (1992), Seismic traveltime inversion for 2–D crustal velocity structure, *Geophys. J. Int.*, *108*, 16–34, doi:10.1111/j.1365-246X.1992.tb00836.x.

Zelt, C. A., and D. J. White (1995), Crustal structure and tectonics of the southeastern Canadian Cordillera, *J. Geophys. Res.*, *100*, 24,255–24,273, doi:10.1029/95JB02632.